Silicon (2014) 6:247–255
DOI 10.1007/s12633-014-9221-3

ORIGINAL PAPER

^{1}H and ^{29}Si NMR Spectroscopy as a Powerful Analytical Tool to Evaluate the Activity of Various Platinum-Based Catalysts in Model Olefin Hydrosilylation

Valérie Meille · Marie-Line Zanota · Fernande Da Cruz-Boisson · Cécile Chamignon · Sébastien Marrot

Received: 15 October 2013 / Accepted: 26 June 2014 / Published online: 30 July 2014

Abstract The structure of polysiloxane copolymers obtained by hydrosilylation of 1-octene with polymethylhydrosiloxane (PMHS) was analyzed by ^{29}Si NMR spectroscopy and revealed a tendency to form block copolymers. Although all the platinum catalysts that were used showed a tendency to form some block structures, only Karstedt catalyst led to well defined block copolymers. However, the tacticity of these copolymers could not be determined using Heteronuclear Multiple Bond Correlation (HMBC) 2D (^{1}H/^{29}Si) NMR technique. The following criteria were found to affect the structure of the hydrosilylation product: low SiH conversion, the "age" of the Karstedt catalyst (low TON) and high octene/SiH ratios.

Keywords Microstructure · PMHS · Hydrosilylation · ^{29}Si NMR · Neighboring effect · Tacticity

V. Meille (✉) · M. -L. Zanota
Laboratoire de Génie des Procédés Catalytiques UMR 5285 CNRS, CPE Lyon, Institut de Chimie de Lyon, Université de Lyon, 43 bd du 11 novembre 1918, BP 82077, 69616 Villeurbanne cedex, France
e-mail: vme@lgpc.cpe.fr

M. -L. Zanota
e-mail: mlz@lgpc.cpe.fr

F. Da Cruz-Boisson
CNRS, UMR 5223, Ingénierie des Matériaux Polymères, Service RMN Polymères, INSA de Lyon, Institut de Chimie de Lyon, Université de Lyon, 69621, Villeurbanne, France
e-mail: fernande.boisson@insa-lyon.fr

C. Chamignon
CNRS, FR 3023, Service RMN Polymères, Institut de Chimie de Lyon, 69622, Villeurbanne, France
e-mail: cecile.chamignon@insa-lyon.fr

S. Marrot
Bluestar Silicones France, 85 avenue des Frères Perret, 69192 Saint-Fons, France
e-mail: sebastien.marrot@bluestarsilicones.com

1 Introduction

Olefin hydrosilylation is one of the most common chemical reactions of the silicone industry [1]. It is generally catalyzed by a platinum catalyst. The actual limits concerning this reaction have been recently reviewed by Troegel et al. [2]. These challenges include issues related to the catalyst itself, immobilization of the platinum catalyst on a solid support [3–6], synergetic interactions with other metals to increase the catalyst activity [2, 7] and also replacing platinum with another metal [2, 8]. In their review about the actual limits in olefin hydrosilylation, Troegel et al. highlighted incoherences in published results, showing the need to study further the mechanism of the reaction [2]. The homogeneous platinum-catalyzed reaction is assumed to proceed through the Chalk-Harrod mechanism, which explains the functionalization of one single SiH unit. In contrast, very few publications are available concerning the detailed structure of the silicone oils obtained from hydrosilylation of olefins with polymethylhydrosiloxane (PMHS) containing several neighboring SiH units: is there a regio and/or stereoselectivity? Concerning the stereoselectivity (tacticity of the polymer), Saxena et al. [9] have found that ^{1}H NMR signals of hydromethylsiloxane units showed a sensitivity to tacticity (meso, racemic) effects. They concluded that there is a preference for racemic orientation

of SiH on PDMS-co-PMHS backbone during hydrosilylation reactions resulting in syndiotactically enriched products.

Concerning the regioselectivity, Kuwae et al. [10] have concluded that the functionalization of SiH units proceeds according the Bernoullian statistics, where the silylation reaction proceeds randomly on the polymeric molecule. Their experiments concerned the hydrosilylation of styrene and the analyses were performed at rather high conversion (72 %). On the other hand, Cancouet et al. found that the hydrosilylation of allyl glycidyl ether involves two neighboring SiH groups [11]. They proposed the formation of a platinum dimer that catalyzes simultaneously the transformation of two neighboring SiH groups. However, their experiment was focused on a specific conversion (50 %) of SiH. Based on their ^{29}Si NMR methodology [12], we used 1-octene over a wide range of octene/SiH ratios and also various platinum catalysts to determine whether the hydrosilylation proceeds via block transformations or via an isolated functions transformation. The configuration of the polysiloxane copolymers was also studied using model compounds.

2 Experimental

2.1 Chemicals

The hydrosilylation reaction studied is shown in Scheme 1. The PMHS is called $MD^{H}_{50}M$, the final product is a polymethyloctylsiloxane (PMOS), $MD^{oct}_{50}M$, where M stands for trimethylsiloxane, D^{H} for hydrogenmethylsiloxane and D^{oct} for methyloctylsiloxane. 1-octene and $MD^{H}_{50}M$ were provided by Bluestar Silicones. A pure $MD^{H}_{50}D_{25}M$ copolymer (PDMS-co-PMHS), where D stands for dimethylsiloxane, was also provided by Bluestar Silicones and was used for NMR studies (Scheme 2).

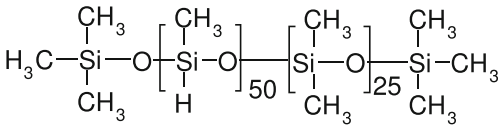

$MD^{H}_{50}D_{25}M$

Scheme 2 $MD^{H}_{50}D_{25}M$ copolymer

2.2 Catalysts

The catalysts have been classified according to two categories: the Karstedt platinum (Platinum(0)-1,3-divinyl-1,1,3,3-tetramethyldisiloxane complex solution, provided by Bluestar Silicones, called "Pt Karstedt", Scheme 3a and the non-Karstedt types. The second category contains the following materials: 1wt-% Pt/C (Johnson Matthey), 1wt-% Pt/PS-DVB (prepared according to [5]), "Pt-NHC" (1,3-Dicyclohexyl-1,3-dihydro-2H-imidazol-2-ylidene)(1,1,3,3-tetramethyl-1,3-divinyldisiloxane)platinum [13], provided by Bluestar Silicones, Scheme 3b and a colloidal suspension of Pt in toluene, named "Colloids", prepared by reduction of platinum dibenzylideneacetone, according to [14].

2.3 Hydrosilylation Reaction

The hydrosilylation reaction was carried out in a glass reactor equipped with a glass impeller and baffles. Octene/SiH ratios were varied from 0.1 to 25, and the platinum content in the final mixture was in the range [1-50ppm]. Samples were regularly collected and analyzed.

In the range of octene/SiH ratios from 1 to 25, 1-octene and the platinum catalyst were initially mixed in the reactor at a regulated temperature of 75 °C. $MD^{H}_{50}M$ PMHS was then added to the mixture at a flow rate of 0.3 mL/min to control the exothermic reaction. For the lower octene/SiH

Scheme 1 Hydrosilylation of 1-octene with PMHS

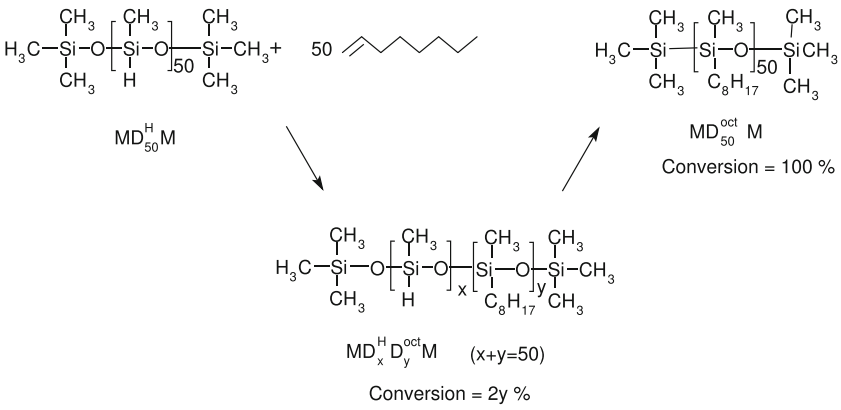

Scheme 3 Homogeneous catalysts - **a** Pt Karstedt - **b** Pt-NHC

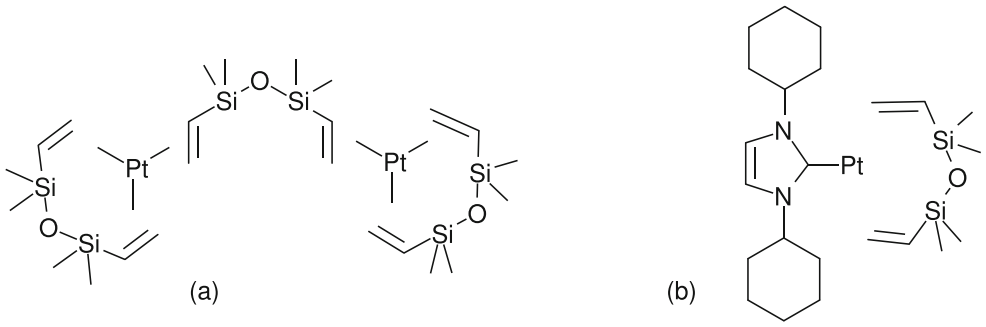

ratios in the range 0.1 to 1, a mixture of 1-octene and PMHS was added to a toluene solution (or suspension) of the platinum catalyst at a regulated temperature of 75 °C and at a flow rate of 1 mL/min, under an inert atmosphere.

2.4 Analytical Methods

2.4.1 ^{1}H *NMR Spectroscopy*

Proton NMR spectra were recorded in deuterated chloroform solutions at 300K using a Bruker Avance III spectrometer (^{1}H: 400.13 MHz). Chemical shifts are referenced to TMS using the chloroform protonated solvent residue as internal standard (7.26 ppm).

2.4.2 2D (^{1}H/^{29}Si*) NMR Spectroscopy*

The ^{1}H/^{29}Si gradient enhanced heteronuclear multiple-bond correlation experiment (g-HMBC) was recorded in deuterated chloroform solutions at 300K using a Bruker Avance III spectrometer operating at 400.13 MHz for ^{1}H and 79.49 MHz for ^{29}Si. The spectrometer was equipped with a 5 mm broad band probe including fluorine observation. Typically 4096 data points with 24 scans for each of 512 t1 increments were acquired. The required acquisition time was 0.51 s and a recycle delay of 5 s was used. Delay to suppress one bond Si-H correlations ($^{1}J_{SiH} = 200$ Hz) was 3.45 ms and delay to allow long range correlations ($^{n}J_{SiH} = 10$ Hz) was 65 ms. Gradients for coherence selection are applied in the ratio 5:5:2. Data was zero-filled to 4096 x 2048 points during data processing.

The ^{1}H/^{29}Si g-HMBC decoupled experiment was created by adding a silicon decoupling block during proton acquisition to the classical gHMBC pulse program. Data was collected under the same conditions as the non decoupled experiment except for the number of scans, reduced to 16 scans per increment.

Fig. 1 ^{29}Si NMR spectrum of reaction mixture

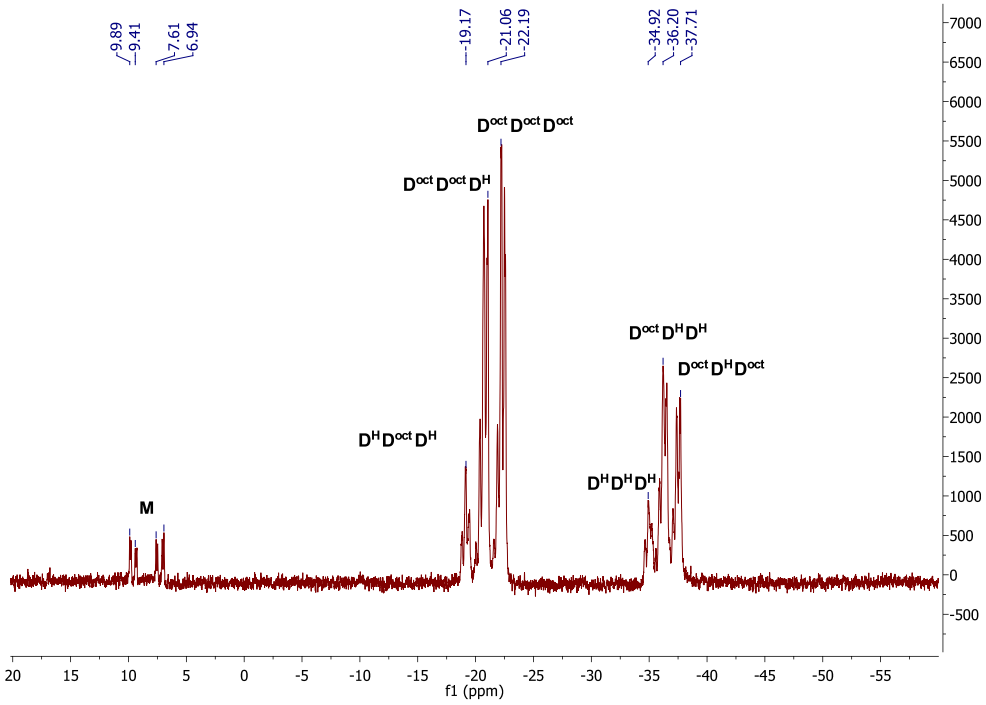

2.4.3 ^{29}Si *NMR Spectroscopy*

Measurement method ^{29}Si NMR spectra were recorded with a Bruker Avance III 400 spectrometer, using TMS as an external standard. The sample was a 80 % solution in deuterated benzene with 1 % iron acetylacetonate to minimize the relaxation time. The deuterium signal was used for the lock and to shim the magnet. 512 scans were collected with 90 degrees pulse angle and 5s delay to allow full relaxation. Decoupling was done only during acquisition using Bruker zgig sequence.

Methodology processing During the functionalization of a PMHS, the influence of the neighbor units on the chemical shift of a given silicon atom leads to triad (and pentad) effects, as reported for co-polymers [12]. A typical spectrum showing the triads is given in Fig. 1.

If the functionalization follows a Bernoullian statistical repartition, a D^{oct} unit can have a D^{oct} unit or a D^{H} as a first neighbor and the same choice as a second neighbor. The probability of getting the different triads at a SiH conversion of X % is:

$$p_{(D^H D^{oct} D^H)} = \left(\frac{1-X}{100}\right)^2 \tag{1}$$

$$p_{(D^{oct} D^{oct} D^H)} = p_{(D^H D^{oct} D^{oct})} = 2 \times \frac{X}{100} \times \frac{1-X}{100} \tag{2}$$

$$p_{(D^{oct} D^{oct} D^{oct})} = \left(\frac{X}{100}\right)^2 \tag{3}$$

This leads to the triad selectivities shown in Fig. 2. It can also be plotted according to the triad yields (see Fig. 3).

The experimental triad proportions or yields can be plotted in comparison with the statistics. Another way to characterize the distribution of the different units is the determination of mean block length and the persistence ratio, fully

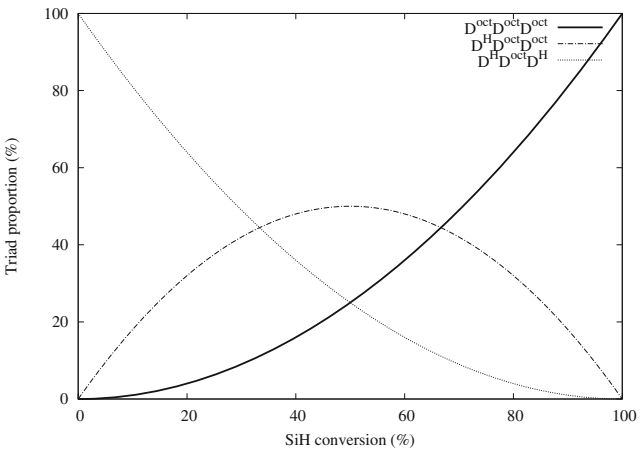

Fig. 2 Statistical triad proportions (selectivities) vs. SiH conversion

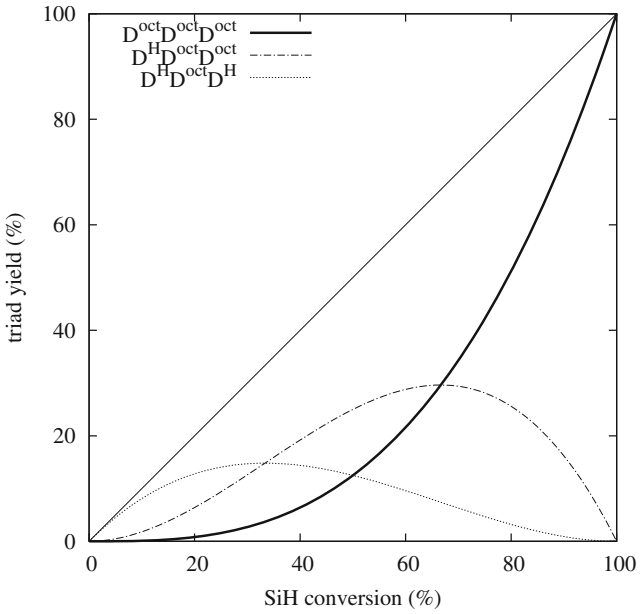

Fig. 3 Statistical triad yields vs. SiH conversion

described and explained by Cancouet et al. [12] and summarized below. The number-average length of a D^{oct} block is the mol fraction of D^{oct} divided by the proportion of $D^{oct}D^{H}$ dyads.

$$L_{D^{oct}} = \frac{[D^{oct}]}{D^{oct} D^H} \tag{4}$$

As $D^{oct}D^{H} = D^{H}D^{oct} = D^{H}D^{oct}D^{H} + 1/2D^{oct}D^{oct}D^{H} = D^{oct}D^{H}D^{oct} + 1/2D^{H}D^{H}D^{oct}$, then:

$$L_{D^{oct}} = \frac{D^{oct} D^{oct} + D^{oct} D^H}{D^{oct} D^H} \tag{5}$$

The experimental number-average length of a D^{oct} block is:

$$L^{exp}_{D^{oct}} = \frac{[D^{oct}]}{D^H D^{oct} D^H + \frac{1}{2} D^{oct} D^{oct} D^H} \tag{6}$$

The number-average length of a D^{oct} block for a random functionalization is:

$$L^{random}_{D^{oct}} = \frac{1}{[D^H]} \tag{7}$$

The persistence ratio η is defined by:

$$\eta = \frac{L^{exp}_{D^{oct}}}{L^{random}_{D^{oct}}} = \frac{[D^{oct}][D^H]}{D^H D^{oct} D^H + \frac{1}{2} D^{oct} D^{oct} D^H} \tag{8}$$

For a random functionalization of the PMHS, $\eta = 1$, for a regularly alternated functionalization, $\eta < 1$. If a neighboring effect is observed, η is much higher than 1. To check the reliability of our NMR analysis, we have analyzed the ^{29}Si NMR spectrum of the $MD^{H}_{50}D_{25}M$ copolymer, which

is expected to show a random distribution of its monomer units [12]. The calculation of η, in which expression D has replaced D^{oct}, gives $\eta = 1.03$, indicating a random occurrence of the D^H and D entities in the copolymer.

3 Results

3.1 PDMS-co-PMHS Analysis for Stereochemistry Issues

3.1.1 Analysis of ^{1}H *NMR Spectra*

The ^{1}H spectrum focusing around the methyl chemical shifts region from 0 to 0.25 ppm is shown for the copolymer $MD^H_{50}D_{25}M$ in Fig. 4.

The presence of several peaks in the methyl region was attributed by Cancouet et al. [12] to a composition effect (influence of the neighboring functions on the methyl proton chemical shift) with a main splitting due to a triad effect. More recently, Saxena et al. [9] proposed an additional sensitivity of those ^{1}H chemical shifts to tacticity based on 2D $^1H/^{29}Si$ g-HMBC experiments. In our opinion, their interpretation for the observed split in the contour, claimed to be related to configurational effects, has to be revised and is mainly due to $^1H - ^{29}Si$ spin-spin coupling in the g-HMBC experiment. Further 2D NMR analysis were performed to discuss this topic.

3.1.2 Analysis of the Detailed Microstructure from 2D NMR Spectra

Heteronuclear Multiple Bond Correlation (HMBC) experiments allow finding connectivities between protons and silicon atoms that are separated by two or more bonds whereas one-bond correlations are suppressed. Nevertheless, the one-bond coupling responses are not always fully suppressed by the sequence and often appear in the long-range correlation spectra. As a consequence, decoupling is rather not used in g-HMBC experiments, and the large doublets due to the one-bond $^1H - ^{29}Si$ coupling (^1J around 200 Hz) can easily be identified. On the contrary, when decoupling is performed, these signals can overlap with long range correlations. Saxena et al. [9] mentioned six cross peaks in the proton methyl region of D^H units when performing classical nondecoupled g-HMBC experiments on PDMS/PHMS copolymer solutions. These resolved cross peaks (three or two resolved cross peaks depending on the ^{29}Si chemical shift) were separated by 0.2 to 0.3 ppm in the ^{1}H axis.

To try to understand this correlation dots mutiplicity, we performed two $^1H - ^{29}Si$ g-HMBC experiments on a $CDCl_3$ solution of $MD^H_{50}D_{25}M$ copolymer, one with a non-decoupled sequence (hmbcgplpndqf) and another one with a sequence which includes a silicon decoupling block during proton acquisition. Several zooms of the obtained correlation maps in the methyl regions of both D and D^H units are shown in Fig. 5. For both experiments, the correlation dots were obtained with an optimized resolution in the ^{29}Si dimension which allows to confirm the previous assignment of split methyl ^{1}H signals of D and D^H units to compositional triad and even pentad effects [12]. When no decoupling is added to the pulse sequence, for one silicon chemical shift value, all the correlations appear as multiple dots: two signals for methyl protons of D units resulting from $^2J^1H - ^{29}Si$ coupling with a measured value in the range 7-8 Hz ($\approx$ 0.2 ppm). For methyl protons of D^H units, those two signals were split again into four correlation peaks coming from a long range $^3J^1H - ^1H$ coupling

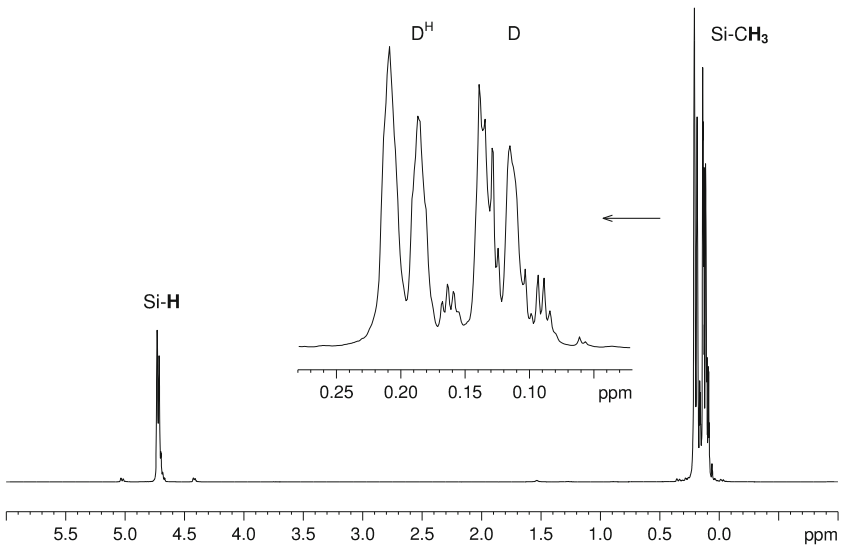

Fig. 4 ^{1}H NMR spectrum of $MD^H_{50}D_{25}M$ copolymer ($CDCl_3$, 300K)

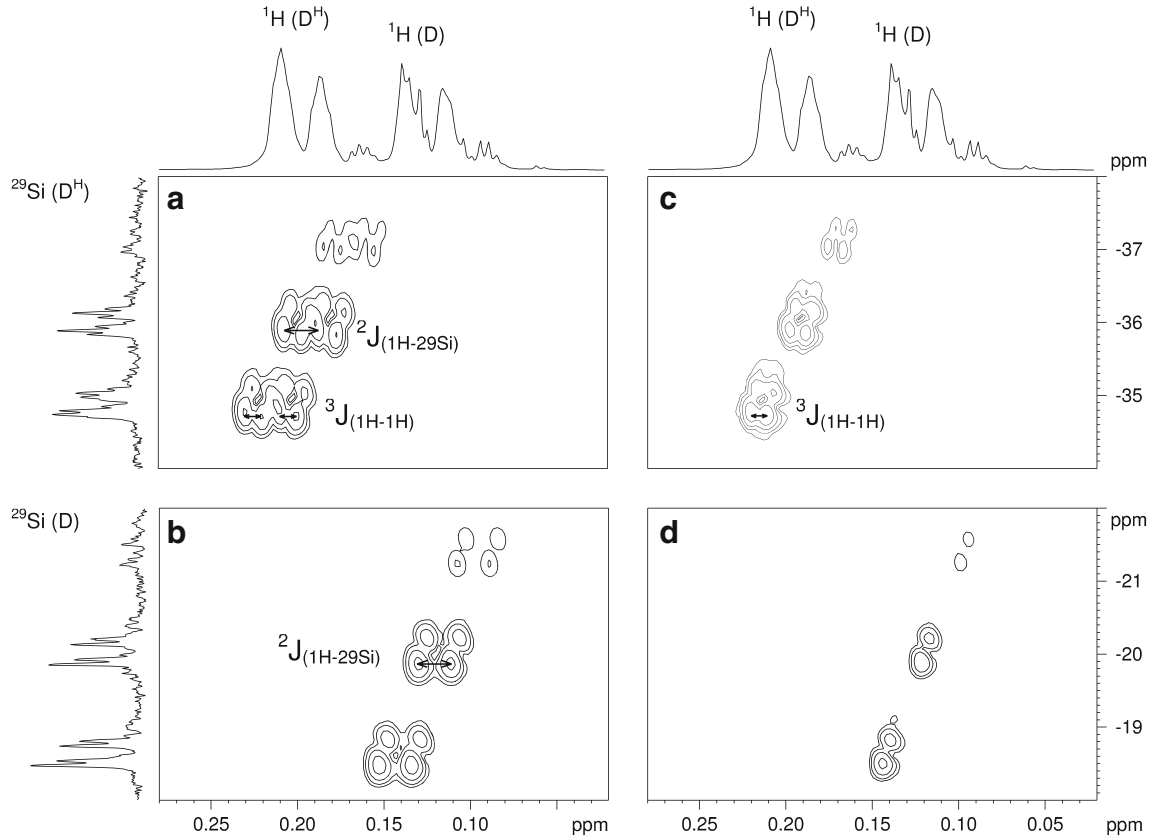

Fig. 5 **a** D^{H} region and **b** D region of $^{1}H/^{29}Si$ non decoupled HMBC; **c** D^{H} region and **d** D region of $^{1}H/^{29}Si$ decoupled HMBC

between Si-CH_3 and Si-H protons ($^{3}J^{1}H - {}^{1}H$ in the range 3-4 Hz). When the silicon decoupling block was added to the sequence, no more splitting was observed in the ^{1}H axis for protons of D units and only a long range $^{1}H - {}^{1}H$ coupling remained for ^{1}H of D^{H} units. This observation confirms that the correlation dots multiplicity observed for nondecoupled g-HMBC experiments cannot be attributed to a stereoisomer resolution.

3.2 Analysis of the Regioselectivity of the 1-Octene Hydrosilylation with PMHS by ^{29}Si NMR

3.2.1 Octene/SiH ratio of 1.4

A standard hydrosilylation reaction was performed with various catalysts, with a small excess of octene (octene/SiH ratio of 1.4). Data was obtained for each of the platinum catalysts at different concentrations and for different reagents composition leading to variation in the yields. The ^{29}Si NMR spectra of all the samples were analyzed in terms of triad occurrence. Analyzing first the occurrence of the $D^{H}D^{oct}D^{H}$ triad, which should be the primary product in a successive sequence $D^{H}D^{H}D^{H} \rightarrow D^{H}D^{oct}D^{H} \rightarrow D^{oct}D^{oct}D^{H} \rightarrow D^{oct}D^{oct}D^{oct}$, a strong deviation from the Bernoullian statistics is observed (in Fig. 6). This means that at low conversion, $D^{H}D^{oct}D^{H}$ is not the primary product as polyfunctionalized PMHS also appears in the initial stage of the reaction. The transformation does not follow

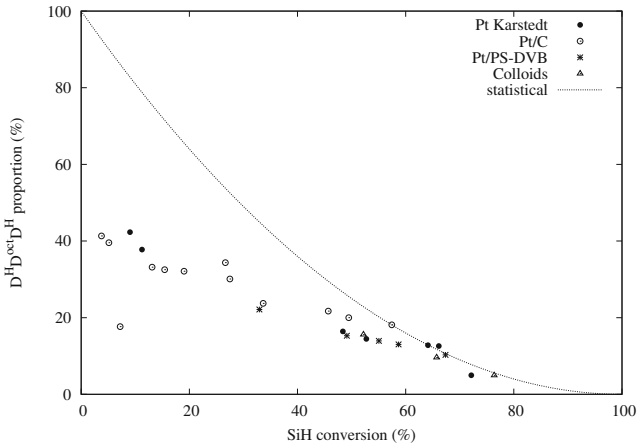

Fig. 6 Selectivity of the $D^{H}D^{oct}D^{H}$ triad for octene/SiH ratio = 1.4

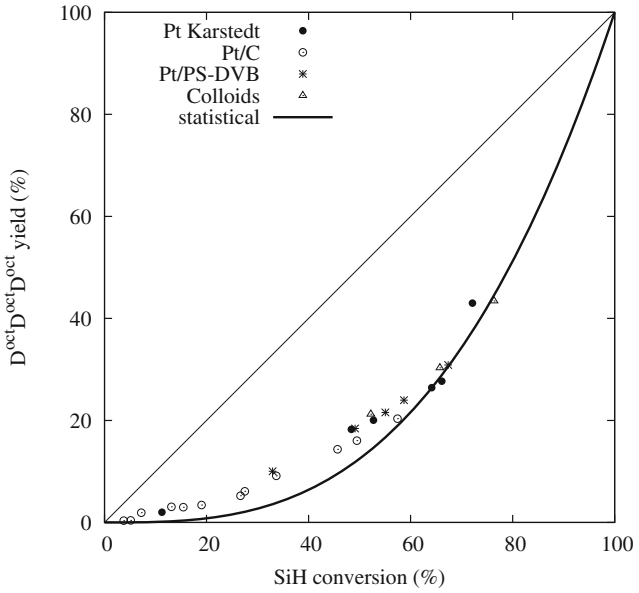

Fig. 7 Yield of the $D^{oct}D^{oct}D^{oct}$ triad for octene/SiH ratio = 1.4

strict successive pathways. Besides, looking at the occurrence of $D^{oct}D^{oct}D^{oct}$, a smaller but noticeable deviation from the Bernoullian statistics is again seen (in Fig. 7). This indicates that trifunctionalized triads can appear as primary products, at the early stage of the reaction. No distinction was observed between the various catalysts tested.

The similar results obtained for the different catalysts were not expected. Actually, the activity of the different catalysts varies to a large extent. It was not expected that their functionalization would occur in the same way. Figure 8 shows the performances of five catalysts, obtained by plotting the SiH conversion calculated from the ^{1}H NMR analysis of samples taken at different times after the end of PMHS addition. The five catalysts were tested at similar concentrations of ca. 11 ppm of platinum in the reaction mixture. The homogeneous catalysts (Pt Karstedt and Pt-NHC) and the colloids are the most active for the 1-octene hydrosilylation. The lowest apparent activity of the supported catalysts (Pt/PS-DVB and Pt/C) can partly be due to mass transfer limitations. Even if the full conversion was not reached during these experiments, the general tendency of the curves indicate that the catalysts were not completely deactivated and could lead to completion. Other experiments, to be published, indicate that 100 % conversion can be reached with the colloidal catalyst at only 7ppm Pt concentration.

To try to further distinguish the catalysts, more experiments were performed at various octene/SiH ratios.

3.2.2 Variation of Octene/SiH Ratio

Many experiments were performed by varying the nature of the catalyst and the octene/SiH ratio from 0.2 to 30. Selected results obtained at 12±2 % SiH conversion are presented in Table 1.

It appears that at low octene/SiH ratio, the persistence ratio η is the lowest, but as said previously, is nevertheless higher than 1 (see entries 1 and 2). For a same catalyst (Pt Karstedt, entries 2-4), η increases with the octene/SiH ratio. The selectivity in $D^{oct}D^{oct}D^{oct}$ obviously also varies in the same way. Different catalysts at similar octene/SiH ratios do not show the same η value (entries 4-6). The Pt Karstedt catalyst shows the highest selectivity in $D^{oct}D^{oct}D^{oct}$

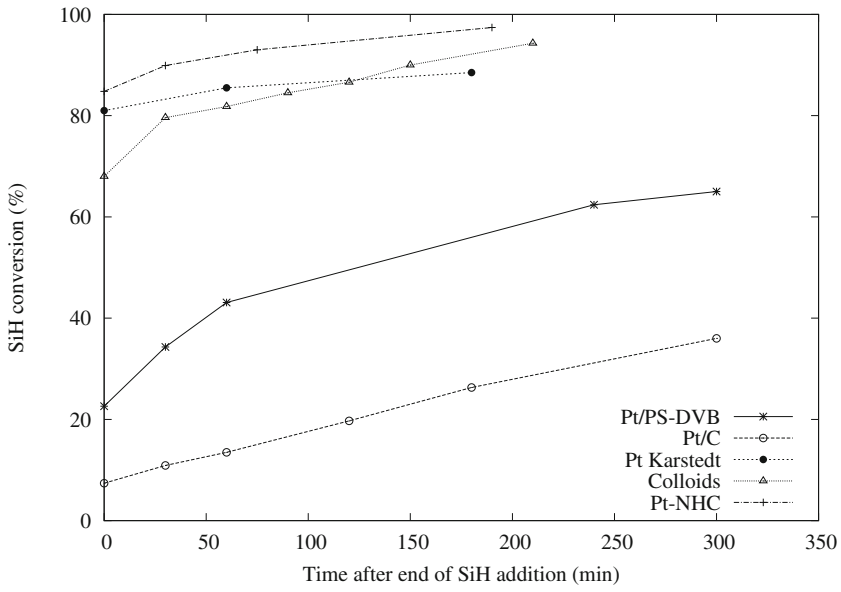

Fig. 8 SiH conversion vs. time after SiH addition for various catalysts (Pt amount is ca. 11 ppm) at octene/SiH ratio = 1.4

Table 1 η and selectivity in $D^{oct}D^{oct}D^{oct}$ obtained at 12 % conversion for various catalysts and R(Oct/SiH)

Entry	Catalyst	R(Oct/SiH)	η ±0.2	Selectivity in $D^{oct}D^{oct}D^{oct}$
1	Pt/C	1.9	1.4	16
2	Pt Karstedt	1.4	1.4	18
3	Pt Karstedt	4.7	2.5	32
4	Pt Karstedt	13.7	5.2	76
5	Pt colloids	15	2.1	34
6	Pt-NHC	16	1.9	27
7	Pt-NHC	30	1.9	30
8	Pt/PS-DVB	12.5	2.1	34

and consequently the highest η. $D^{oct}D^{oct}D^{oct}$ even seems to be a primary product for the Karstedt catalyst when the octene/SiH ratio is high.

More results, obtained at various conversions, were recorded on a same graph plotting η versus the SiH conversion (Fig. 9). The Karstedt catalyst is represented by dots (•) and all the other catalysts are represented by plus signs (+). The octene/SiH ratio is represented by the grayscale. As far as the Karstedt catalyst is concerned, its "age" was also found to impact the microstructure of the product. The age was accounted by the turnover number (TON = moles of SiH converted by moles of Pt) represented by varying the point size (size decreasing when the TON increases). Some example values of the TON were inserted on the graph, just above the corresponding point.

The first result is that, whatever the catalysts (dots and plus signs), all the experiments carried out at octene/SiH ratio between 0.1 and 1.5 (light gray) show a very moderate block effect, with persistence ratios varying from 1 to 2. At higher octene/SiH ratios (dark points), the behavior of the Karstedt catalyst (•) becomes singular, with persistence ratios reaching values higher than 10. Another singular aspect of the Karstedt catalyst is its ability to show various behaviors depending on its age. Very high persistence ratios are obtained at low SiH conversion and only for wide and dark dots. The highest values of η are thus obtained for the Karstedt catalyst when the three following conditions are simultaneously met: low SiH conversion, fresh catalyst (low TON, wide dots) and high octene/SiH ratios (dark dots).

Obtaining different behaviors for Karstedt and non-Karstedt catalysts seems to imply at least two different reaction mechanisms: one for the fresh Karstedt catalyst, and one for all the other catalysts. It is believed that the Karstedt catalyst is rapidly transformed to colloids, thus explaining the singular behavior of the sole fresh catalyst.

Colloids have been suspected to be the active species of the Karstedt catalyst for a long time [15]. A more recent paper has demonstrated that the active species of the Karstedt catalyst was not a colloidal catalyst but a monomeric platinum compound with silicon and carbon in the first coordination sphere [16]. On the contrary, the unique behavior of Pt-NHC has been described by Marko et al. [13, 17] since the discovery of this catalyst and it was clearly established that no colloidal species were formed during its mode of action. Based on these studies, Pt-NHC was expected to

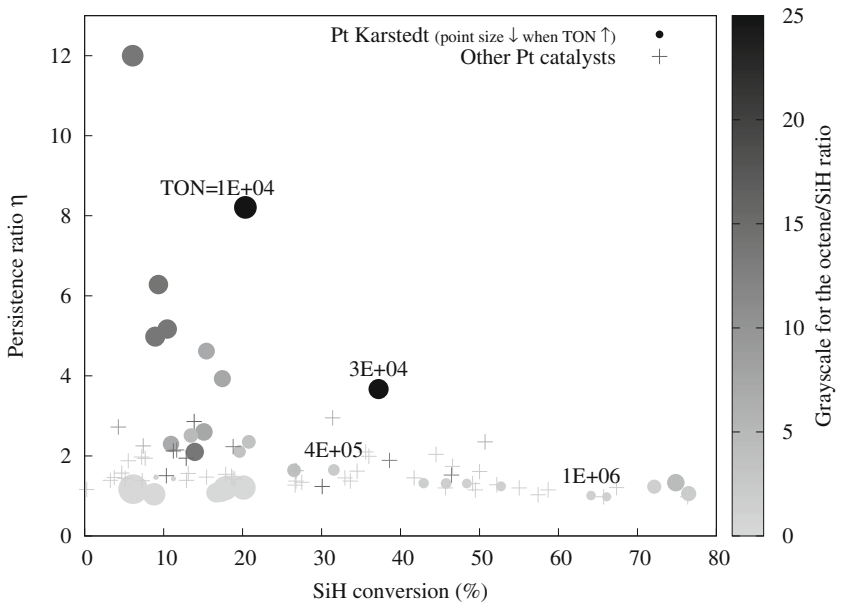

Fig. 9 Persistence ratio η versus SiH conversion, for different octene/SiH ratio (grayscale), different catalysts (Pt Karstedt • and all others +) and different catalyst ageing (point size). TON = moles of converted SiH functions per mole of platinum

give different results from the other catalysts, namely the platinum nanoparticles and the Karstedt one. The singular behavior of the Karstedt catalyst (and not Pt-NHC), with a pronounced neighboring functionalization, is surprising.

Cancouet et al. [11] reported a similar neighboring effect observed with the Speier catalyst (hexachloroplatinic acid hexahydrate in isopropyl alcohol) during the hydrosilylation of allylglycidylether with poly(methylhydrosiloxane-co-dimethylsiloxane). Dyads were found to be much more reactive than isolated units, which was tentatively explained by the simultaneous insertion of two vicinal SiH groups in a binuclear complex of platinum. A similar explanation could partially justify the results reported here, but would be in contradiction with the published assumption that the active species in the Karstedt catalyst are mononuclear [16]. Moreover, not only two adjacent SiH groups are involved in our hydrosilylation of 1-octene but more, as shown by the initial abundance of the $D^{oct}D^{oct}D^{oct}$ triad. Our ongoing work concerns a tentative mechanism to explain the singular behavior of the Karstedt catalyst. It should imply the insertion of a second and neighboring SiH group before the reductive elimination of the first functionalized siloxane. Such a mechanism is perhaps not favoured for the Pt-NHC catalyst due to the steric hindrance of the substituted imidazolyl ligand. This could explain the different behavior of both homogeneous catalysts. More work is needed to go further.

4 Conclusion

1D and 2D NMR analyses (^{29}Si and ^{1}H) of polymethylhydrosiloxanes allowed to reach the following conclusions: 1) no information about the tacticity of the polymer is available from such analyses, 2) a block functionalization of the PMHS is observed during the 1-octene hydrosilylation. Such neighboring effect that was observed for all the platinum catalysts was more pronounced for Karstedt catalyst which appears to indicate that there is no single reaction mechanism for all the various hydrosilylation catalysts.

Acknowledgments This work was carried out in the framework of the French ANR program CP2D "HEXOSIC" (2008-2012). Most of the 1D ^{29}Si NMR data were obtained in the CCRMN of Lyon.

References

1. Marciniec B (2009) Hydrosilylation: a comprehensive review on recent advances. Springer
2. Troegel D, Stohrer J (2011) Recent advances and actual challenges in late transition metal catalyzed hydrosilylation of olefins from an industrial point of view. Coord Chem Rev 255(13–14):1440–1459
3. Hofmann M, Eberle HJ (2006) Platinum catalysts that are supported on nanoscale titanium dioxide, use thereof in hydrosilylation, hydrosilylation method using said catalysts and compositions comprising said catalysts. WO Patent WO2006061138
4. Alonso F, Buitrago R, Moglie Y, Ruiz-Martinez J, Sepulveda-Escribano A, Yus M (2011) Hydrosilylation of alkynes catalysed by platinum on titania. J Organomet Chem 696(1):368–372
5. Wawrzynczak A, Dutkiewicz M, Gulinski J, Maciejewski H, Marciniec B, Fiedorow R (2011) Hydrosilylation of n-alkenes and allyl chloride over platinum supported on styrene-divinylbenzene copolymer. Catal Today 169(1):69–74
6. Schmid G, West H, Mehles H, Lehnert A (1997) Hydrosilation reactions catalyzed by supported bimetallic colloids. Inorg Chem 36(5):891–895
7. Klein K, Knott W, Windbiel D (2000) Synergistic catalyst system and method for carrying out hydrosilylation reactions. Patent EP1031603
8. Tondreau AM, Atienza CCH, Weller KJ, Nye SA, Lewis KM, Delis JGP, Chirik PJ (2012) Iron catalysts for selective anti-markovnikov alkene hydrosilylation using tertiary silanes. Science (New York, NY) 335(6068):567–570
9. Saxena A, Markanday M, Sarkar A, Yadav VK, Brar AS (2011) A systematic approach to decipher the microstructure of methyl hydrosiloxane copolymers and its impact on their reactivity trends. Macromolecules 44(16):6480–6487
10. Kuwae Y, Kushibiki N (1989) NMR study on microstructure of polymer produced by hydrosilation of styrene with poly(hydrogenmethylsiloxane). J Polym Sci Part A: Polym Chem 27(12):3969–3975
11. Cancouet P, Pernin S, Helary G, Sauvet G (2000) Functional polysiloxanes. II. neighboring effect in the hydrosilylation of poly(hydrogenmethylsiloxane-co-dimethylsiloxane)s by allylglycidylether. J Polym Sci Part A: Polym Chem 38(5):837–845
12. Cancouet P, Daudet E, Helary G, Moreau M, Sauvet G (2000) Functional polysiloxanes. i. microstructure of poly(hydrogenmethylsiloxane-co-dimethylsiloxane)s obtained by cationic copolymerization. J Polym Science Part A: Polym Chem 38(5):826–836
13. Marko IE, Sterin S, Buisine O, Mignani G, Branlard P, Tinant B, Declercq JP (2002) Selective and efficient platinum(0)-carbene complexes as hydrosilylation catalysts. Science 298(5591):204–206
14. Pelzer K, Hvecker M, Boualleg M, Candy JP, Basset JM (2011) Stabilization of 200-atom platinum nanoparticles by organosilane fragments. Angew Chem Int Ed 50(22):5170–5173
15. Lewis LN, Lewis N (1986) Platinum-catalyzed hydrosilylation - colloid formation as the essential step. J Am Chem Soc 108(23):7228–7231
16. Stein J, Lewis LN, Gao Y, Scott RA (1999) In situ determination of the active catalyst in hydrosilylation reactions using highly reactive pt(0) catalyst precursors. J Am Chem Soc 121(15):3693–3703
17. Buisine O, Berthon-Gelloz G, Briere JF, Sterin S, Mignani G, Branlard P, Tinant B, Declercq JP, Marko IE (2005) Second generation n-heterocyclic carbenePt(0) complexes as efficient catalysts for the hydrosilylation of alkenes. Chem Commun 30:3856–3858